HYDRATION AND N-ACETYL-L-CYSTEINE ALTER THE MICROSTRUCTURE OF HUMAN NAIL AND BOVINE HOOF: IMPLICATIONS FOR DRUG DELIVERY.

Nogueiras-Nieto. L.[a], Gómez-Amoza J.L.[a], Delgado-Charro M.B.[b] and Otero-Espinar F.J.[a]

[a] Departamento de Farmacia y Tecnología Farmacéutica. University of Santiago de Compostela, Campus Vida s/n, 15782 Santiago de Compostela, Spain.
e-mail: luisnogs@gmail.com, joseluis.gomez.amoza@usc.es, Francisco.otero@usc.es .

[b] Department of Pharmacy and Pharmacology, University of Bath, Claverton Down, Bath, BA2 7AY, UK.
e-mail: B.Delgado-Charro@bath.ac.uk

Corresponding author: M. B. Delgado-Charro
Department of Pharmacy and Pharmacology, University of Bath,
Claverton Down, Bath, BA2 7AY, UK.
e-mail: B.Delgado-Charro@bath.ac.uk
Phone: +44 (0) 1225 383969
Fax: +44 (0) 1225 386114

Abstract:

This work aimed to (a) characterize the microstructure and porosity of human nail and bovine hoof by mercury intrusion porosimetry and SEM image analysis, (b) study the effects of hydration and of N-acetyl-l-cysteine treatment on the microstructure of both membranes, and (c) determine whether the microstructural modifications were associated with changes in drug penetration measured by standard diffusion studies. Bovine hoof surface is more porous than nail surface although there were no differences between the mean surface pore sizes. Hydration and N-acetyl-l-cysteine increased the roughness and apparent surface porosity, and the porosity determined by mercury intrusion porosimetry of both membranes. Pore-Cor™ was used to generate tridimensional structures having percolation characteristics comparable to nail and hooves. The modeled structures were horizontally banded having an inner less-porous area which disappeared upon treatment. Treatment increased the predicted permeability of the simulated structures. Triamcinolone permeation increased significantly for hooves treated N-acetyl-l-cysteine, i.e., the membranes for which microstructural and permeability changes were the largest. Thus, microstructural changes determined via mercury intrusion porosimetry and subsequently modeled by Pore-Cor™ were related to drug diffusion. Further refinement of the technique will allow fast screening of penetration enhancers to be used in ungual drug delivery.

Keywords: nail, hydration, N-acetyl-l-cysteine, microstructure, porosity, intrusion porosimetry

Introduction

Human nails cover and protect the dorsal aspect of the terminal phalanges of fingers and toes. Nails increase sensory perception at the finger pads, facilitate object manipulation and contribute to temperature regulation. Thus, nail changes, deformities, and loss cause both functional problems as well as aesthetically alterations [1,2]. Changes to the nail structure result from a variety of conditions: trauma, fungal, bacterial and viral infections and dermatological disorders like psoriasis and lichen planus. The most frequent of these being mycosis and psoriasis [2-4]. Current treatment of onychomycosis and nail psoriasis include oral and topical pharmacological treatment and nail avulsion as last choice [2-4]. Topical therapy is highly desirable due to its localized effects, it minimizes adverse systemic effects, avoids drug interactions (an important concern with oral antifungal therapy) and potentially improve adherence. However, due to the nature and structure of the nail plate, mainly constituted by keratin, drug permeability across the nail is severely limited, hindering the effectiveness of topical therapies [2-5].

The nail plate presents the main barrier to ungual penetration; this 0.5-1.0 mm thick structure results from a keratinization process during which: (a) the cells become flattened, their organelles and nuclei degenerate and the cytoplasma is filled with keratin fibrils embedded in a protein matrix, (b) a cellular envelope resistant to protease action is formed and (c) the intercellular space is filled with material discharged from membrane coating granules [1,6-7]. Fetal nail precursor cells only express skin type (soft) keratin but adult nail precursor cells modify this pattern to express predominantly hair type (hard) keratin (ventral nail matrix); however some limited areas present co-expression of hair and skin keratins (apical nail matrix) and some only of skin keratins (dorsal and apical nail matrices) [8]. The different contribution of these areas to the formation of the layers of the nail plate explains some of their properties [1,9-12]. Thus, the dorsal nail plate derives primarily from the dorsal nail matrix and is rich in calcium, phospholipid and sulphydryl groups and has little acid phosphatase activity. The largest, intermediate layer of the nail plate derives mainly from the ventral nail matrix and has a high acid phosphatase activity, low calcium, low phospholipid and low bound sulphydryl group content but a high number of disulphide bonds groups. Finally the ventral layer which consists of 1-2 layers of cells is provided by the nail bed and share similarities with the dorsal (calcium, phospholipid and sulphydryl groups) and with the intermediate (high acid phosphatase activity and disulphide bonds) layers. The three layers also differ in the dimensions of the corneocytes which are flatter in the dorsal than in the intermediate layer and the intercellular zones which have ampular dilatations in the dorsal layer and anchoring knots in the intermediate layer [1,10-11].

About 38-45% of a keratin molecule has an α-helix conformation kept by hydrogen bonds, and disulfide intrapeptide bonds. Keratin molecules associate into heterodimers, tetramers and into protofilaments and protofibrils which finally form the keratin filaments [12]. These low-sulphur proteins belong to the intermediate filament family of proteins and are embedded in a non-filamentous matrix made of high sulfur proteins (rich in cysteine) and high glycine/tyrosine proteins which is an intermediate-filament associated protein. This highly ordered filament-matrix structure is stabilized via disulphide bonds and provides effective mechanical and barrier properties. Hard cornified structures like the nail have higher content of sulfur (cysteine and methionine) than the stratum corneum, nevertheless 20% of the keratine heterodimers of the nail are skin (soft) type. Another difference is the keratin filament associated proteins which are trychohyalin and trychoplein for the hard keratins and profilaggrin and filaggrin for the soft type. Keratin filaments are connected to the cornified envelope and to desmosomes and hemidesmosomes which provides resistance to the nail structure [12].

The rigidity, thickness and hardness of the nail plate provide excellent protection for the sensitive finger tips. Unfortunately, these properties make topical drug delivery extremely difficult. Drug permeation into the nail plate occurs via passive diffusion and is restricted by this highly cross-

linked plate structure. On the other hand, the physicochemical properties of the permeants also determine their rate and extent of nail penetration. Drug permeation across the nail plate is mostly influenced by the active molecular weight, while the role of its lipophilicity seems minor [13-15].

Different strategies have been proposed to increase nail permeation of drugs either by altering the plate barrier using penetration enhancers or by physical methods [4,14-15]. Some thiol compounds such as N-acetyl-l-cysteine, 2-mercaptoethanol, N-(2-mercaptopropionyl) glycine, and thioglycolic acid break the disulphide bonds present in the nail plate. This structural disruption of the nail plate probably results in formation of new pores interconnected by transport channels and the increased network of channels would facilitate drug penetration. In other words, it is expected that these penetration enhancers would induce noticeable changes in the microstructure of the nail plate. However, this has not been completely demonstrated to date. Hydration of the nail plate increases ungual permeation of some drugs [4,14-16] supposedly by softening and increasing the flexibility of the nail plate which once swollen would allow drugs to diffuse more easily. However, hydration-induced changes to the nail microstructure have not been unequivocally demonstrated.

Bovine hooves have been used regularly used as an alternative to human nail in permeation studies. However, hooves have been reported to be more permeable than human nail plate due to their less dense keratin matrix [17,18]. Further, hoof proteins have significantly less cystine residues, and most likely fewer disulphide links than human nail [19,20]. Thus, enhancers such as N-acetyl-l-cysteine which act by breaking keratin disulphide bonds could have different impact upon nail plate and bovine hooves.

Mercury intrusion porosimetry has been employed to characterize the microstructure of different solid materials and informs about the total porosity, pore size distribution, pore connectivity and tortuousness of porous materials [21,22]. This information can be used to predict the topology of porous structures using geometric models of various complexities [23-27]. The Pore-Cor™ software is based on the cylindrical- or cubic-shaped pores model. This useful tool has been employed very frequently to model porous structures since it also predicts liquid permeation across the sample tested [28-29]. Complementary information is provided by image analysis of scanning electron microscopy (SEM) microphotographs which has been used to analyze the surface structure of materials [22,30-31].

A first aim of this work was to study the effects of hydration and of the penetration enhancer N-acetyl-l-cysteine on the microstructure of human nails and bovine hoof membranes by using mercury intrusion porosimetry and image analysis of SEM-microphotographs. The results will provide further evidence about the mechanism by which water and the N-acetyl-l-cysteine promote drug permeation across the nail. A second objective was to compare the microstructure of hoof and human nail membranes as revealed by the two techniques as well as their relative susceptibility to water and N-acetyl-l-cysteine.

Materials and Methods:

1. Materials.

Nail tip samples were obtained from fingers and toes of healthy volunteers, aged between 25–50 years who cut their own nails after giving informed consent. The samples were carefully cleaned and washed with water, dried at room temperature and stored in a glass container at room temperature. The nail samples used for permeation studies had a minimum 8 mm length while those used for all other studies ranged 1-3 mm approximately.

Bovine hoof was obtained from the local abattoir (Compostelana de Carnes S.L., Santiago de Compostela, Spain). The hooves were cleaned, washed and frozen. Subsequently, the samples were thawed and soaked in water during 24 hours to facilitate their cutting (Ufesa Professional Slicer FS50) into thin slices (0.3-0.7 mm thickness) which were dried at room temperature and then stored frozen.

N-acetyl-l-cysteine (AC) and Pluronic F-127 (poloxamer 407) were obtained from Sigma-Aldrich Chemical Co. (Madrid, Spain) and triamcinolone acetonide (TA) was purchased from Fagron Iberica (Barcelona, Spain). Methyl-beta-cyclodextrin (MβCD with a molar substitution of 0.57 and a MW 1191 Da, Kleptose Crysmeb) were from Roquette-Laisa (Barcelona, Spain). Potassium dihydrogen phosphate, sodium chloride, sodium azide and ammonium acetate analytical grade were from Panreac Química S.A. (Barcelona, Spain), dodecahydrate sodium dihydrogen phosphate, potassium chloride and acetonitrile (HPLC grade) were from Merck (Germany).

2. Nails and membrane hoof treatment.

"Test samples" of human nail and bovine hoof were prepared by combining specimens from different individuals and hooves to a final mass of approximately 0.6 g. These 0.6 g test samples of either nail clips or bovine hoof slices were soaked in 10 mL of either water or 10% N-acetyl-l-cysteine aqueous solution and stored at ambient temperature for a maximum of 5 days. Nails and hooves were removed after 24, 48 and 120 hours of treatment, frozen by immersion in liquid nitrogen and freeze-dried (Labconco Corp.,USA) at -30ºC for 48 hours to eliminate water.

3. SEM analysis.

Untreated and 48 h and 120 h treated nail and bovine hoof samples were mounted on double-sided tape on aluminum stubs and micrographs were taken using a Leo VP-435 SEM (Leo Electron Microscopy, UK). Images were taken of either surface of the hooves and of the dorsal surface of the nail. Some nails were transversally cut to image the cross-section of the nail by SEM. To perform surface analysis 1.024x768 grey scale images were stored in TIFF format which allowed for a 256-level intensity scale. The pore size distribution at the nail and hoof surfaces were estimated using the grain analysis modulus of the SPIP 4.6.0 software package (Image Metrology A/S, Denmark). An automatic threshold was used to convert grey scale to binary images.

4. Mercury intrusion porosimetry (MIP) and pore modeling.

Untreated and treated nail and hoof samples were analyzed using a Micromeritics 9305 pore sizer (Norcross GA, USA) fitted with a 3-mL powder penetrometer and working pressures in a 0.004–172.4 MPa range. The amount of either nail or hoof used for each test was approximately 0.6 grams. The pore size data were used for modeling the porous structure of the samples as simulated porous networks using Pore-Cor™ 6.11 software (Environmental and Fluid Modelling Group, University of Plymouth, UK). Pore-Cor™ generates a three-dimensional void structure having percolation characteristics as close as possible to those of the material experimentally characterized by MIP. The modeling assumes the material to consist of interconnected unit cells of 1000 pores (of arbitrary cubic shape) arranged in a regular three-dimensional 10×10×10 array and connected by up to 3000 throats (of arbitrary cylindrical shape) [21,32-34]. The pore coordination number ranges from 1 (one throat per pore) to 6 (each pore is connected to 6 neighbor pores by throats); the connectivity being defined as the arithmetic mean of the pore coordination number over the unit cell. In each unit cell, the centers of the pores are equidistant to each other; the distance being the pore range spacing, Q. Thus, each unit cell is a cube-like structure possessing 10 Q length sides [29,32]. Connecting throats are generated to have sizes between the greatest and the lowest pore diameters (i.e., between d_{max} and d_{min}) experimentally

obtained by MIP. The throat size distribution is fitted to a log-normal distribution with a throat skew, q, ranging from −50 (distribution skewed to d_{min}) to 50 (skewed to d_{max}). Each cubic pore has a size equal to the size of the greatest throat connected to the pore multiplied by a pore skew, which has values ranging from 1 to d_{max}/d_{min} [29,32]. Throats and pores are arranged in the unit cell according to the value of the correlation level. This parameter has values between 0 (random spatial arrangement) and 1 (maximum banding or other structuring of the unit cell) [21,32,33]. The modeling process starts by placing the throats in the unit cell. Next, 1000 pores are placed so each one is connected to neighbor pores by at least one throat. The modeling continues by increasing or diminishing the value of Q, i.e., changing the size of the unit cell and enlarging or shortening throats, to bring the porosity of the modeled structure close to the experimental value. The mercury intrusion process in the unit cell is simulated by Pore-Cor™ which subsequently compares the simulated "pore size *versus* volume" curve to that experimentally obtained (in both cases normalized porosities are used). The distance parameter "f" provides the mean distance between the data points of the experimental and the simulated intrusion curves, thus indicating the goodness of the fitting. Because the X-axis of those plots is logarithmic and the Y-axis includes normalized porosity data, f is also normalized and adimensional. Values of f close to or smaller than 1 indicate that the simulated model truly represents the behavior of the real material [33]. The Boltzmann-annealed simplex algorithm was used to estimate and simultaneously optimize the connectivity (mean number of throats per pore), pore skew, throat skew and correlation level from the mercury intrusion porosimetry cumulative curves [33]. The modeling process also considered that: (i) the resulting structure of the unit cell should fit to the experimental porosity avoiding the overlapping of pores; (ii) there are not closed pores; and (iii) the geometric parameters are actually or potentially verifiable by experimental data [33].

Finally, the permeability (k) of the simulated structures for nail and hooves was modeled assuming that Poiseuille flow (water) occurred in the -z direction according to [21]:

$$k = \frac{\Pi}{8}\omega_{cell}(Farcs)\frac{l_{cell}}{A_{cell}}$$

where l_{cell} and A_{cell} represent the length and the cross-sectional area of the unit cell, respectively and $\omega_{cell}\ (Farcs)$ is an averaging operator over the whole unit cell operating on the flow capacities of the pore-throat-pore arcs parallels to the z-axis. Pore-Cor™ calculated the term $\omega_{cell}\ (Farcs)$ by means of the Dinic network analysis algorithm [34,35].

5. Infrared spectroscopy

IR spectra of treated and untreated nails and bovine hoof samples were obtained on an IR spectrophotometer VARIAN, Model 670 IR using ATR PIKE techniques.

6. Permeation Studies

Either one nail tip or one slice of bovine hoof was sandwiched between two cylindrical adapters (Mecanizados del Noroeste, Santiago de Compostela, Spain) made of Teflon with an O-shaped ring providing an effective diffusional area of 0.785 cm^2. This set was then mounted in vertical Franz-type diffusion cells (Vidrafoc, Barcelona, Spain) having a 5.5 mL receptor volume. Two permeation experiments were performed with hooves; the vehicles were 2 mL saturated solutions of TA in either water or in a 10% AC aqueous solution. One experiment was performed with nails which used a 2 mL saturated solution of TA in a 10% AC, 20% Pluronic F-127 and 10% methyl-beta-cyclodextrin aqueous solution. The donor drug concentration remained practically constant throughout all the permeation studies. The receptor was filled with a pH 7.4 phosphate buffer containing sodium azide (30 mg/L) to prevent algae and microbial growth. 1 mL samples of

the receptor were taken every 24 hours and the volume replaced with fresh buffer. Drug concentration in the receptor medium was quantified by high-performance liquid chromatography (HPLC).

7. TA quantification.

TA concentration was determined by an HPLC method adapted from the literature [36]. A Merck-Hitachi chromatographic equipment was used which consisted of a pump (L-6200), an automatic injector (AS-4000), a column thermostat (L-5025) and a UV detector (Diode-array, model L-4500) connected to a computer by an interface (model D-6000). Briefly, a 55:45 acetonitrile: 20 mM ammonium acetate (pH=5) mobile phase was pumped (0.8 mL/min) through a Waters Symmetry® RP-18 (5 μm, 4.6x150 mm) column kept at 40ºC. TA was detected at 232 nm and its retention time was about 3.5 min. The analytical method was validated for sensitivity, recovery, linearity, accuracy and precision.

Results and discussion

This work aimed to characterize the microstruture of human nails and bovine hoof membranes and to determine whether this microstructure is altered by hydration and by the penetration enhancer N-acetyl-l-cysteine. For this, treated and untreated nail and hoof samples were studied using mercury intrusion porosimetry and image analysis of SEM-microphotographs. It was not possible to source nail plates, typically excised from cadavers, in the relatively large quantities required for the porosimetry tests. Therefore, nail clippings from healthy volunteers were used. Nail clippings correspond to the free edge of the nail (or anterior margin of the nail plate) and are widely used in nail permeation studies. Whether the permeability or other relevant properties differ in the nail plate as it progresses distally has not been ellucidated.

Figure 1.A-B shows SEM images of the surface of untreated nail tips (dorsal layer) and bovine hoof slices at two different magnifications. The dorsal surface of nails appeared dense, compact and smooth surface presenting few small holes and fractures; the x1000 magnification also allowed visualization of the corneocytes of the nail plate. The surface of bovine hoof slices appeared more heterogeneous and irregular; however this could be partially an artifact resulting from the mechanical cut of the hooves.

The SEM microphotographs were used to estimate the superficial porosity and the size distribution of superficial pores via image analysis techniques, using the grain analysis modulus of the SPIP software package. As shown by Figure 2, both untreated nails and hooves present a log-normal surface pore size distribution with geometric mean (geometric standard deviation) values of 10.2 (2.24) and 10.5 (3.2) μm respectively (Table 1). Thus, no differences between the mean surface pore size of untreated nails and hooves were found. On the other hand, the differences observed in the frequency distribution, as shown in Figure 2, indicated the surface of hoof membrane to be more porous than the nail surface. A 48 h treatment with water and AC10% induced significant changes at the surface of the samples; the more obvious alteration was shown by hooves treated with AC10% (Figure 1.D). These observations are consistent with previous data. According to Kobayashi et al. [15] N-acetyl-cysteine assists drug permeation by interacting with the disulphide bridges between keratin molecules thus facilitating nail swelling and softening. Gupchup et al. reported that nails treated with 5% AC swelled ~3 times more than untreated nails [37]. Our SEM images (Figure 1) show that AC10% treatment significantly increased the roughness and the apparent surface porosity of nails and hooves. Possibly, the disruption of disulphide bonds in the keratin matrix facilitated swelling and corneocyte detachment. The surface analysis made by image analysis of the x500 SEM microphotographs allowed estimation of the distribution of the surface pore size. The log-normal distributions found (Figure 2, Table 1) showed an increased frequency distribution which suggests an

important enhancement of the surface porosity for all treated samples, especially in hoof samples treated with AC10%, however neither water nor AC10% modified the mean surface pore size.

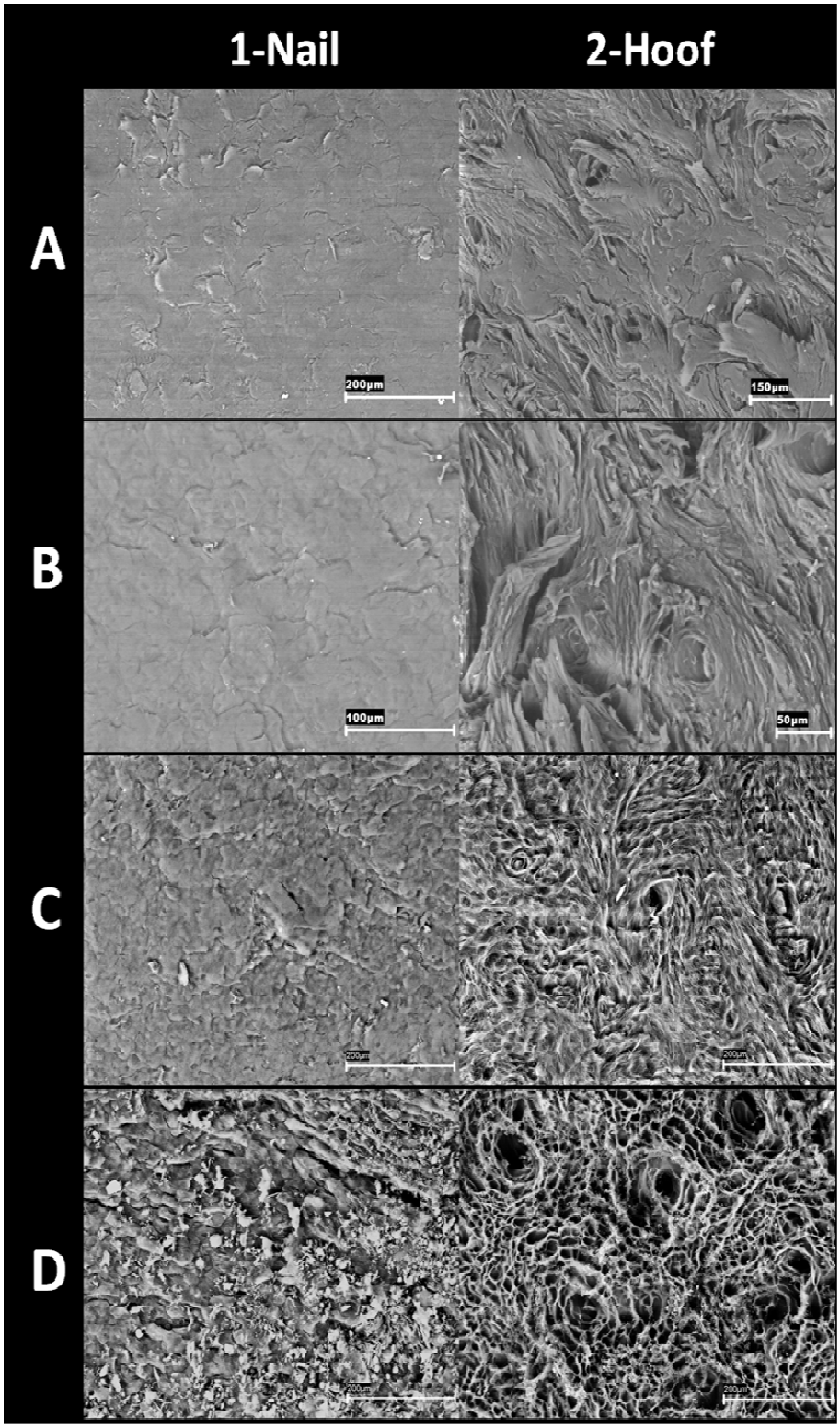

Figure 1. SEM images of the surface of the nail dorsal layer (left column) and of bovine hoof slices (right column): panel A: untreated (magnification x500); panel B: untreated (magnification x1000), panel C: 48 h hydration (magnification x500) and panel D: 48 h - AC 10 % (magnification x500). Bars length is: 200 µm (A.1; C; D), 150 µm (A.2), 100 µm (B.1) and 50 µm (B.2).

Cross section SEM images (figure 3) did not reveal any significant changes in the internal structure of the nail plate caused by hydration. Nevertheless, a 120 h treatment with AC10% caused disruption of the internal structure of the nail. These effects are possibly due to the reasons already discussed. On the whole, these results indicate that both hydration and AC10% treatment promote the formation of pores at surface of the nail plate and bovine hoof.

Table 1. Mean surface pore size estimated for treated and untreated nail and hoof samples. The treatment consisted on incubating the samples with either water or AC10% for 48 h.

Treatment	Nail		Bovine hoof	
	Geometric mean (μm)	geometric standard deviation	Geometric mean (μm)	geometric standard deviation
Untreated	10.2	2.24	10.5	3.2
Water	9.5	2.09	8.4	1.89
AC10%	9.0	1.96	11.32	2.09

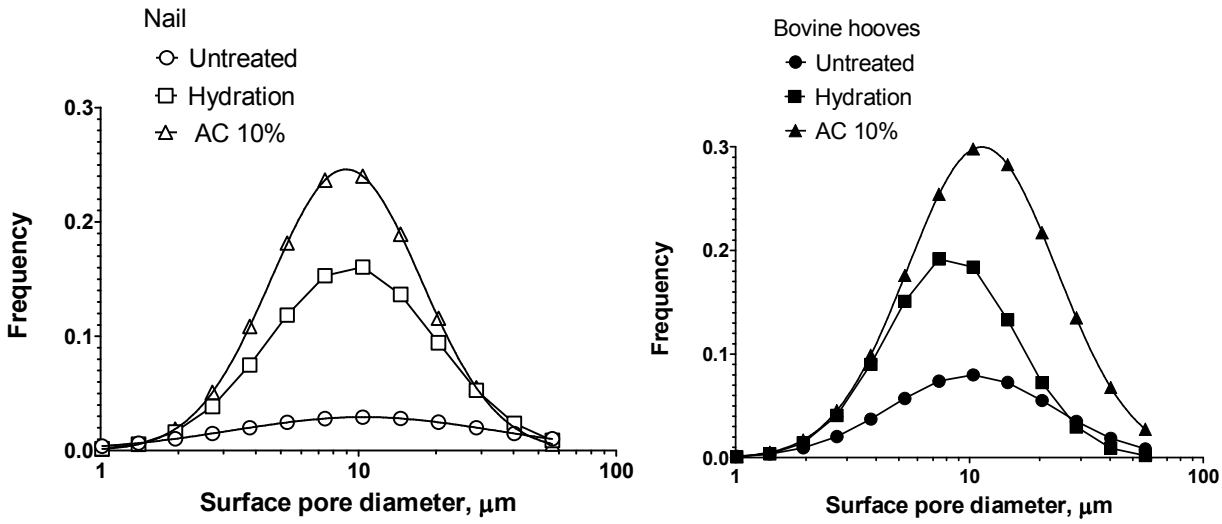

Figure 2. Log-normal size distribution of the surface pores of nails tips and bovine hooves estimated from SEM images. The length of treatment was 48 h.

SEM and image analysis only allow investigation of changes occurring at the surface of the samples, therefore mercury intrusion porosimetry studies were performed to investigate whether hydration or AC10% treatment altered the internal microstructure. The distributions of pore volume corresponding to untreated and treated pore are shown in Figure 4. Untreated nails and hooves show a similar microstructure characterized by very low porosity values. Both hydration and AC10% treatment increased the porosity of both substrates but the effect was more pronounced for hooves and when AC was used. We believe this is the first report on the surface pore size distribution of nails and hooves, on the porosity of nails and hooves, and on the effect which hydration and AC have on the distributions of pore volume of these two substrates.

The pore size distributions determined via MIP were used for modeling the porous structure of the samples using Pore-Cor™ 6.11 software; the f values were lower than 1.15 in all cases thus indicating a good fitting [33]. Figure 5 shows the correlation level obtained for each model and Figures 6 and 7 show the 3-D structure of the unit cell of the optimized models in which holes and pores are represented by cubic spaces interconnected by cylindrical throats (this same shape was also assumed in intrusion mercury analysis [38]). The modeled structures for untreated nail and

hoof are similar: pores and holes are present at the surface of the unit cell but the internal structure has very low porosity. As previously discussed, the correlation level varies between 0 for a completely random structure, and 1 indicating an organization in the unit cell [21]. The correlation levels (Figure 5) obtained for untreated nails (0.805) and hooves (0.81) suggest them to be organized structures, possibly reflecting the two areas presenting different porosity. This kind of microstructure has obvious implications on drug delivery; chemicals would penetrate with relative ease the superficial, more porous layer of the nails but will find increased difficulty to penetrate into and across the internal, less porous structure.

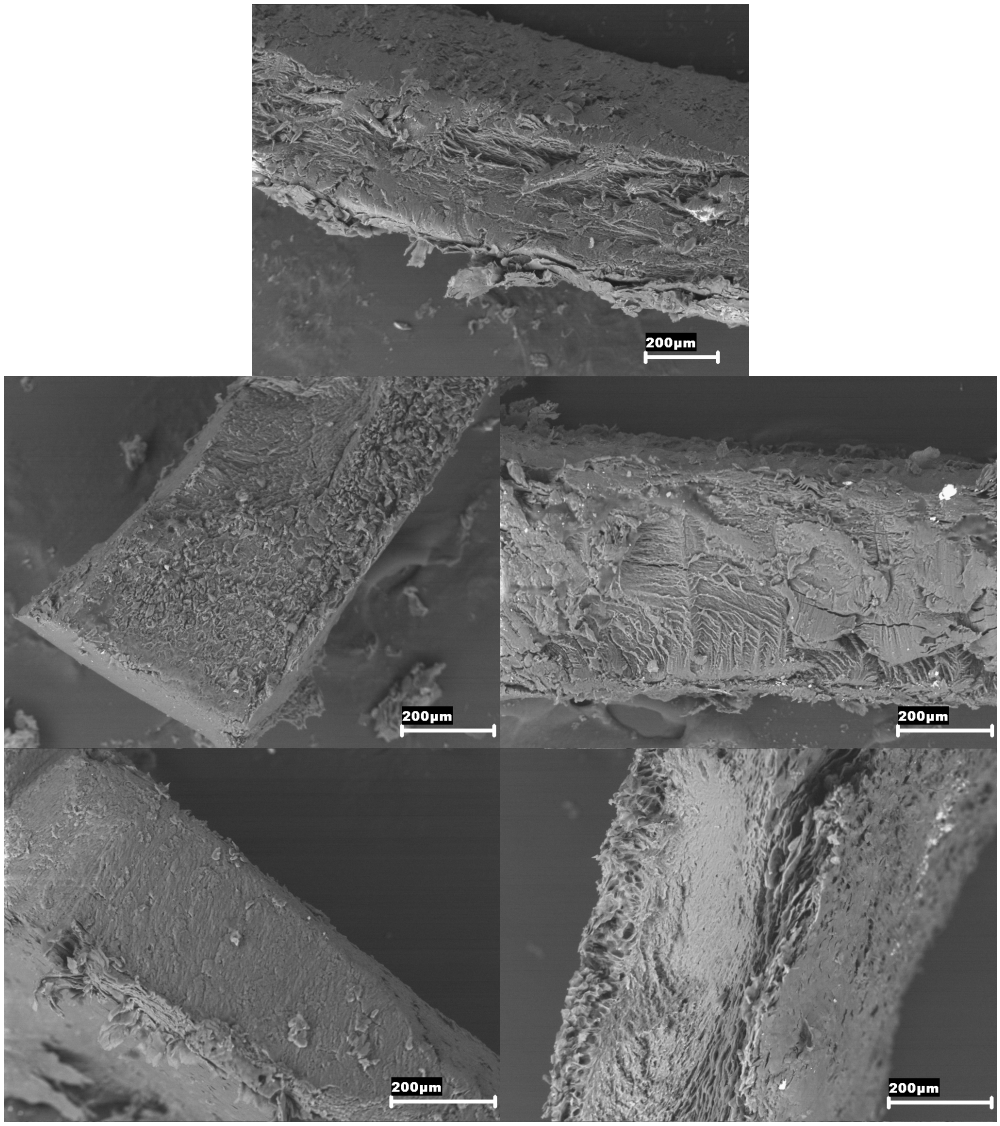

Figure 3. Cross sectional SEM images of nail tips: untreated (upper), 48 h hydration (middle, left), 120 h hydration (bottom, left), AC 10 % during 48 h (middle, right) and AC 10% 120 h (bottom, right).

Hydration modified the porous microstructure of nails and hooves. The decrease in the correlation levels (Figure 5) observed for the hydrated samples indicates the randomization of the structure, i.e., suggests the formation of a more homogenous system. The modeled structures (Figure 6-7) indicated that hydration increased pore size, promoted pore interconnection and decreased the extent of the internal, less porous area. The non-porous internal zone is dramatically reduced for hooves immersed in water for 24 hours, and completely disappears after 120 h. Accordingly, the correlation level observed for these samples is low (Figure 5) which is consistent with the formation of a random structure as result of the

disappearance of the internal non-porous area. The effects of hydration on nail clips are markedly less pronounced, there is a modest increase in porosity and the non-porous central area does not completely disappear even after 5 days of hydration, hence the correlation level decreased less for nails. Overall, these results suggest that nails retained a more organized structure than hooves after similar hydration times. Secondary chemical bonds (principally hydrogen bonds, Van der Waals and electrostatic interactions) play a key role in the interaction between the matrix and filament proteins, contributing to the cohesion of keratin and the physical structure and mechanical properties of nails and hooves [39,40]. Most of the water present in nails is hydrogen bound to proteins; and it has been suggested that an increased water content impacts negatively on these secondary chemical bonds, thus causing some separation between the fiber and matrix proteins and loosening the nail structure [39,40]. Figure 8 shows the FTIR spectra of the nail and hoof before and after treatment; there were no changes observed in spectra of hydrated nails and hooves with respect to untreated samples, indicating that hydration had caused no modification in disulphide links.

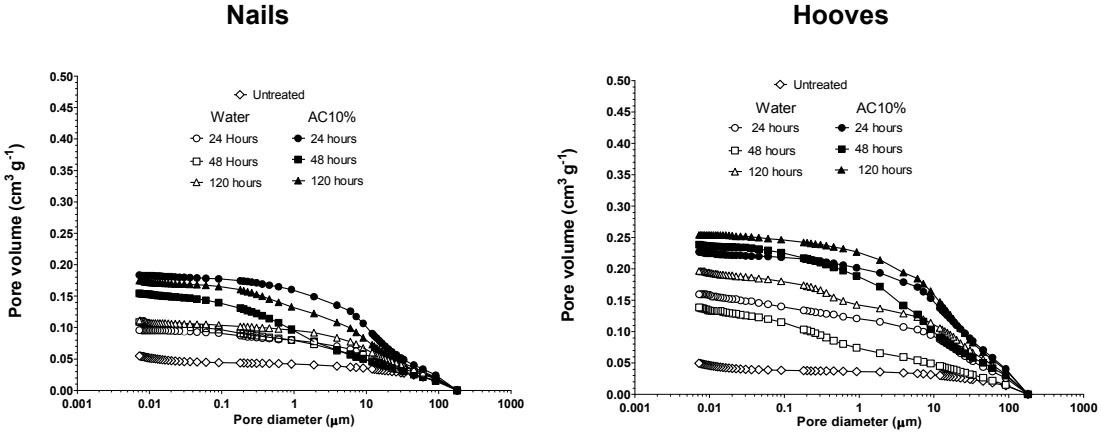

Figure 4. Cumulative curves of mercury intrusion data for treated and untreated for nail (left) and bovine hoof (right).

On the other hand, nails and hooves differ in their cysteine content [19, 20] and in their water uptake and swelling behavior as reported by Khengar et al. [41]. The lower abundance of disulphide bonds in hooves would make them more susceptible to structural changes caused by water interference with secondary bonds and result in increased swelling [41, 19,20].

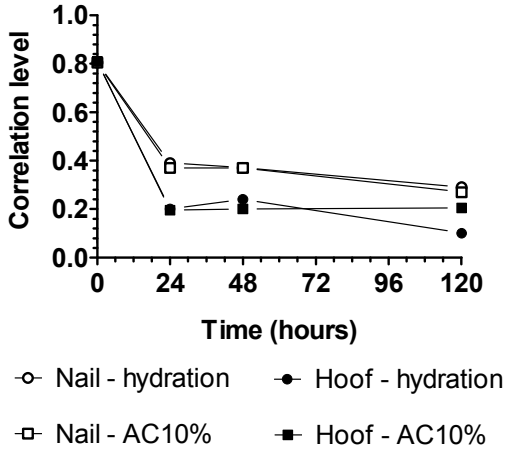

Figure 5. Correlation levels determined for the structural models generated by Pore-Cor™ software for untreated and treated nails and hooves.

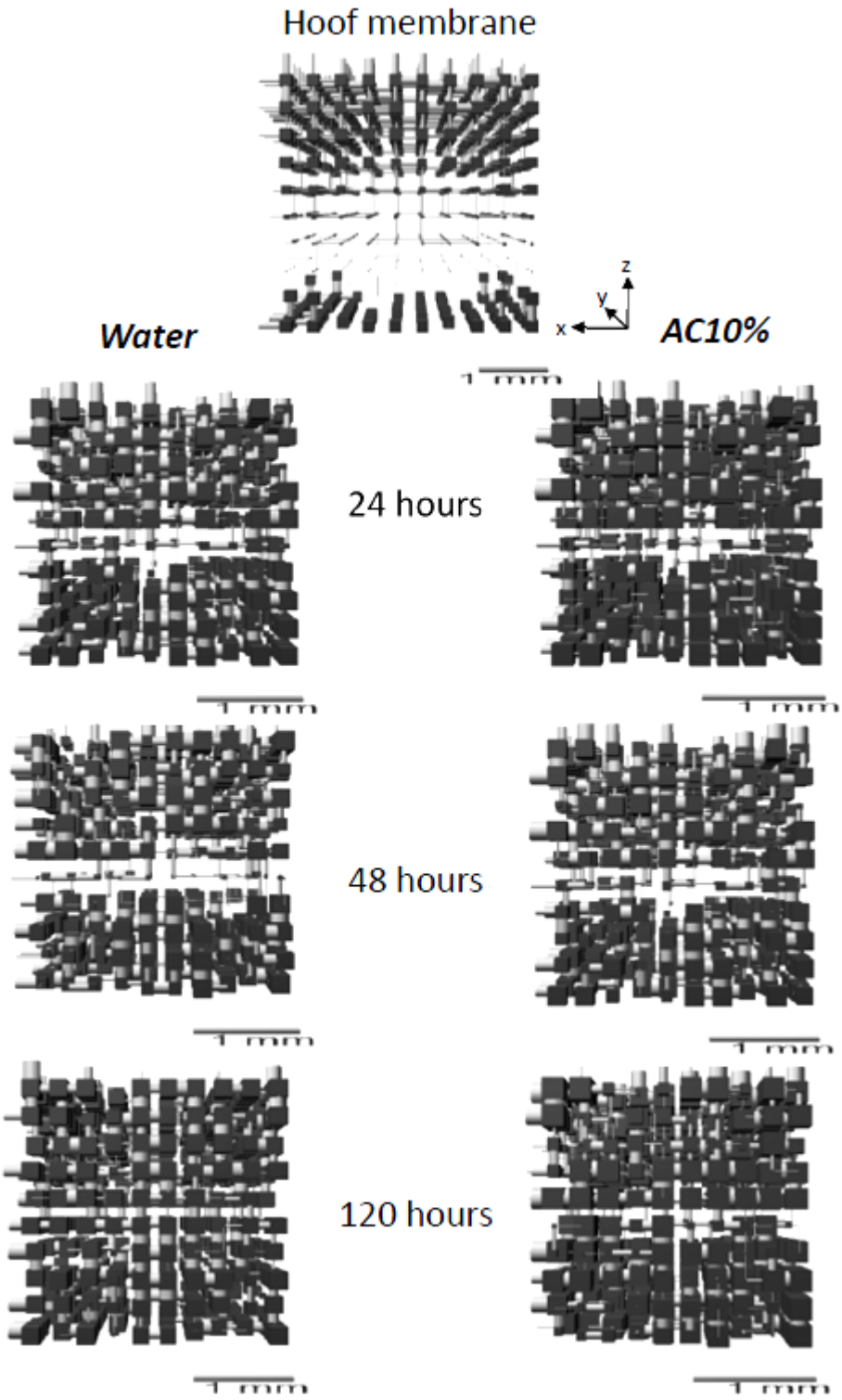

Figure 6. Unit cells of bovine hoof membrane as modeled from mercury intrusion porosimetry data using Pore-Cor™ software: the throats are represented by cylinders and connect the pores which are represented by cubes; the void space between cylinders and cubes corresponds to solid material.

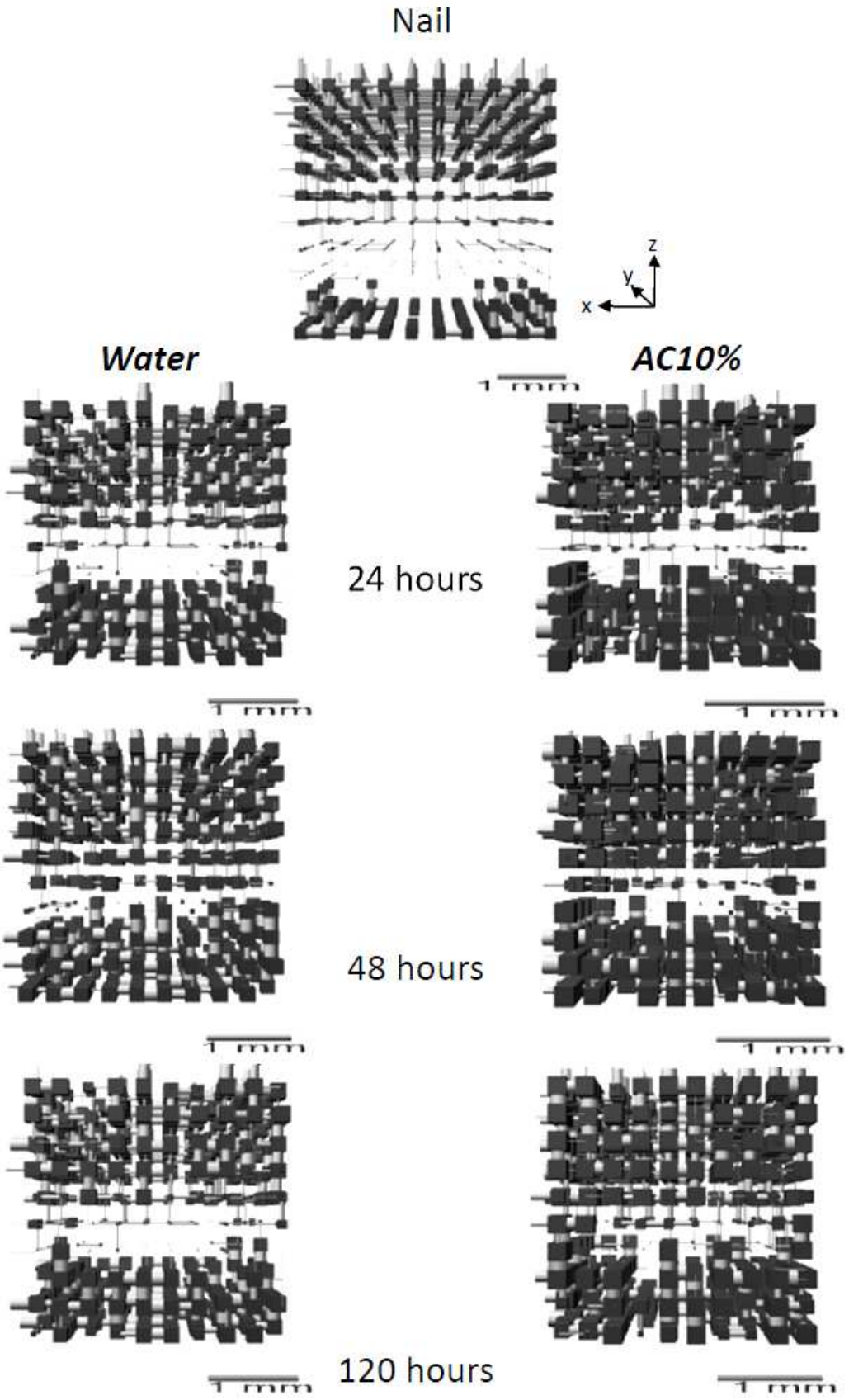

Figure 7. Unit cells of human nail plate as modeled from mercury intrusion porosimetry data using Pore-Cor™ software: the throats are represented by cylinders and connect the pores which are represented by cubes; the void space between cylinders and cubes corresponds to solid material.

Incubation with the AC10% solution produced greater changes in both substrates. The cumulative curves of MIP (Figure 5) and the modeled structures (Figures 6 and 7) illustrate the increase in pore size and connectivity, and the loss of the non-porous central area observed in these samples. The decrease of the correlation levels (Figure 5) indicated that AC treatment resulted in randomization of the structures. The effects caused by the AC10% were more severe than those caused by hydration (Figures 4, 5) and the differences between the modeled structures of hydrated and AC10% treated samples (Figures 6-7) were more noticeable for nails whose structure was less disrupted by hydration. The larger number of disulphide bonds present in nail keratin probably makes nails more sensitive to agents that disrupt disulphide bounds. Our results are consistent with previous data; AC treatment reduces disulphide links [1, 15, 18, 41] facilitating water diffusion and water-protein bonding in the nail which further disrupts the structure by interfering with secondary bounds as previously discussed. Unfortunately, changes in S-S bonds could not be determined by FT-IT due peak interferences with the AC diffused into the nail and hoof. On the other hand, the hoof structure is already significantly altered by hydration. Nevertheless, the largest changes in the permeability predicted by PoreCor™ were for the AC treated hooves. (Figure 9), probably due to the combined effect of hydration and AC in hooves

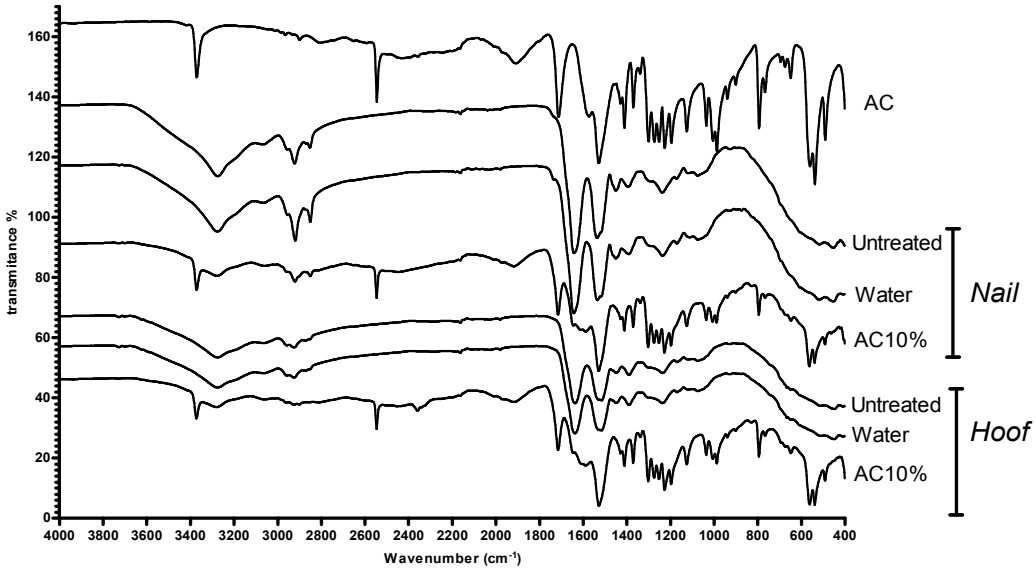

Figure 8. FTIR spectra of nail and hoof membrane untreated and after 120 hours of treatment with water and AC10%.

Figure 9 shows the values of permeability of the simulated structures for nail and hooves predicted by Pore-Cor™. The permeability (k) is a measure of the ease with which a porous material allows fluid to pass through it as defined by Darcy's law [42]. Because the geometry used to represent the microstructure of these systems is very simple compared to that of real nails and hooves, the permeability values should be regarded as a tendency of the percolation characteristics of the systems analyzed [43]. The permeability was increased for both nails and hooves after 24 hours of treatment, the predicted changes were much sharper in the case of hooves treated with 10% AC aqueous solution. Furthermore, longer (48 and 120 h) treatment times would not induce further increments in the permeability of either modeled membrane.

Diffusion experiments were performed to investigate whether the changes observed in the microstructure of nails and hooves can be linked to drug penetration across these membranes.

Triamcinolone acetonide (TA) was selected because this corticoid is commonly used to treat nail psoriasis and a topical, non-invasive therapy would be an attractive alternative [4,14]. TA was not detected in the receptor chamber after 14 days of diffusion when delivered from saturated aqueous solution across hooves. A donor solution containing AC10% resulted in a significant increase of TA delivered across the hoof membrane (the cumulative amounts delivered at 24h, 48h and 120 h were 8.34 µg (±2.36), 20.36 µg (±6.36) and 29.61 µg (±5.48) respectively (mean ± SD, n=3). However, the drug was not detected in the receptor when human nail was used. These results are in good agreement with the structural models here proposed; most precisely with the porosity determined via MIP and the predicted permeability modeled with Pore-Cor™ software (Figures 6, 7, 9). Indeed, the hooves treated with AC10% showed the largest microstructural alterations and increase in permeability which seemed linked to the lower barrier to drug diffusion and higher drug permeation. Unfortunately, no TA fluxes could be measured for the other membranes, which made impossible to establish quantitative correlations between micro structural perturbation and flux enhancement. Diffusion experiments exposed just one side (0.78 cm^2) of the nail and hoof to 2 mL of the donor solution while microstructural changes were investigated in samples completely soaked and incubated in 10 mL of medium. Thus, the effects of water and AC10% were probably reduced during the diffusion experiments. Nevertheless, our results suggest that determination of microstructural changes via MIP and their subsequent modeling by Pore-Cor™ were related to drug diffusion. Further refinement of the technique could be used to quickly screen penetration enhancers for ungual drug delivery.

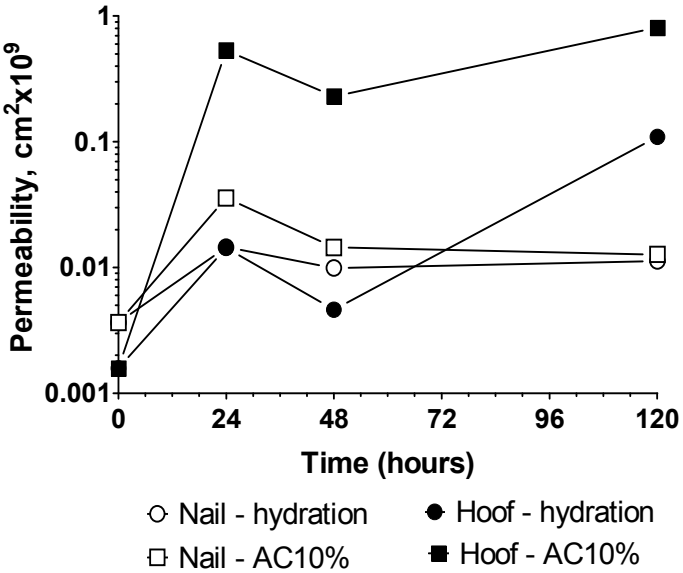

Figure 9. Permeability predicted by PoreCor™ for the modeled structures generated for untreated and treated nails and hooves.

Conclusions

Mercury intrusion porosimetry and SEM imaging can be used to characterize the surface and internal porosity of human nail and bovine hooves as well as the effects of hydration and N-acetyl-l-cysteine on the microstructure of these substrates. The bovine hoof surface is more porous than the nail surface although the mean surface pore size of untreated samples was similar for both substrates. Treatment with water and AC10% increased the apparent surface porosity of nails and hooves as determined by SEM image analysis and the porosity as determined by mercury intrusion porosimetry. Pore-Cor™ software was successfully used to generate tridimensional structures having percolation characteristics comparable to those of nail and hooves. The modeled structures were horizontally banded suggesting the presence of an

internal less porous area, this organized structure disappeared upon treatment with water and N-acetyl-l-cysteine. The predicted permeability of the simulated structures for nail and hooves also increased upon treatment. Triamcinolone permeation increased significantly for hooves treated with N-acetyl-l-cysteine, precisely the membranes for which microstructural and predicted permeability changes were the largest. In conclusion, these results suggest that microstructural changes determined via mercury intrusion porosimetry and subsequently modeled by Pore-Cor™ can be related to drug diffusion across human nail and bovine hoof. The differences between the microstructure of bovine hooves and nail clippings, and their relative alteration by hydration and N-acetyl-cysteine here reported recommend caution when data obtained with this animal model is extrapolated to human nail. Further refinement of the technique will be required to allow fast screening of penetration enhancers to be used in ungual drug delivery.

Acknowledgements

L. Nogueiras Nieto thanks the "Consellería de Industria - Xunta de Galicia" for a studentship.

REFERENCES

[1] D.A.R. De Berker, J. André, R. Baran, Nail biology and nail science, Int. J. Cosmet. Sci. 29 (2007) 241-275.
[2] J. Thomas, G.A. Jacobson, C.K. Narkowicz, G.M. Peterson, G.H. Burnett, C. Sharpe, Toenail onychomycosis: an important global disease burden, J. Clin. Pharm. Ther. 35 (2010) 497-519.
[3] J. Obadiah, R. Scher, Nail disorders: Unapproved treatments, Clin. Dermatol. 20 (2002) 643-648.
[4] S. Murdan, Enhancing the nail permeability of topically applied drugs, Expert Opin. Drug Deliv. 5 (2008) 1267-1282.
[5] S. Kumar, A.B. Kimball, New antifungal therapies for the treatment of onychomycosis, Expert Opin. Investig Drugs. 18 (2009) 727-734.
[6] K. Hashimoto, Ultrastructure of the human toenail. Cell migration, keratinization, and formation of the intercellular cement, Arch. Derm.Forsh. 240 (1971) 1-22.
[7] K. Hashimoto, Ultrastructure of the human toenail. I I Keratinization and formation of the marginal band, J. Ultra. Res. 36 (1971) 391-410.
[8] T. Kitahara, H. Ogawa, Cellular features of differentiation in the nail, Microsc. Res. Techniq. 38 (1997) 436-442.
[9] J.C. Garson, F. Baltenneck, F. Leroy, C. Riekel, M. Müller. Histological structure of human nail as studied by synchroton X-ray, Cell. Mol. Biol. 46 (2000) 1025-1034.
[10] A. Jarrett, R.I.C. Spearman, The histochemistry of the human nail, Arch. Derm. 94 (1966) 652-657.
[11] D. Parent, G. Achten, F. Stouffs-Vanhoof, Ultrastructure of the normal human nail, Am. J. Dermatopathol. 7 (1985) 529-536.
[12] H.H. Bragulla, D.G. Homberger, Structure and functions of keratin proteins in simple stratified and cornified epithelia, J. Anat. 214 (2009) 516-559.
[13] Y. Kobayashi, T. Komatsu, M. Sumi, S. Numajiri, M. Miyamoto, D. Kobayashi, K. Sugibayashi K, Y. Morimoto, In vitro permeation of several drugs through the human nail plate: relationship between physicochemical properties and nail permeability of drugs, Eur. J. Pharm. Sci. 21 (2004) 471-477.
[14] S. Murdan, Drug delivery to the nail following topical application, Int. J. Pharm. 236 (2002) 1-26.
[15] Y. Kobayashi, M. Miyamoto, K. Sugibayashi, Y. Morimoto, Enhancing effect of N-acetyl-l-cysteine or 2-mercaptoethanol on the in vitro permeation of 5-fluorouracil or tolnaftate through the human nail plate, Chem. Pharm. Bull. 46 (1998) 1797-1802.
[16] H.B. Gunt, G.B. Kasting, Effect of hydration on the permeation of ketoconazole through human nail plate in vitro. Eur. J. Pharm. Sci. 32 (2007) 254-260.

[17] R. Elkeeb, A. Alikhan, L. Elkeeb, X. Hui, H.I. Maibach. Transungual drug delivery: Current status, Int J Pharm 384 (2010) 1-8.
[18] D. Mertin, B.C. Lippold, In-vitro permeability of the human nail and of a keratin membrane from human hooves: Prediction of the penetration rate of antimycotics through the nail plate and their efficacy, J. Pharm. Pharmacol. 49 (1997) 866-872.
[19] R.C. Marshall, Genetic variation in the proteins of human nail, J Invest Dermatol. 75 (1980) 264-269.
[20] H.P. Baden, J. Kubilus. Fibrous proteins of bovine hoof, J. Invest Dermatol. 81 (1983) 220-224.
[21] G.M. Laudone, G.P. Matthews, P.A.C. Gane, Modelling diffusion from simulated porous structures, Chem. Engineer. Sci., 63 (2008) 1987-1996.
[22] A. Gómez-Carracedo, C. Alvarez-Lorenzo, R. Coca, R. Martínez-Pacheco, A. Concheiro, J.L. Gómez-Amoza, Fractal analysis of SEM images and mercury intrusion porosimetry data for the microstructural characterization of microcrystalline cellulose-based pellets, Acta Mater. 57 (2009) 295-303.
[23] J.M. Zalc, S.C. Reyes, E. Iglesia, Monte-Carlo simulations of surface and gas phase diffusion in complex porous structures, Chem. Engineer. Sci. 58 (2003) 4605-4617.
[24] J.M. Zalc, S.C. Reyes, E. Iglesia, The effects of diffusion mechanism and void structure on transport rates and tortuosity factors in complex porous structures, Chem. Engineer. Sci. 59 (2004) 2947-2960.
[25] J. Kloubek, Investigation of porous structures using mercury reintrusion and retention, J. Colloid Interface Sci. 163 (1994) 10-18.
[26] J. Wood, L.F. Gladden, Modelling diffusion and reaction accompanied by capillary condensation using three-dimensional pore networks. Part 1. Fickian diffusion and pseudo-first-order reaction kinetics, Chem. Engineer. Sci. 57 (2002) 3033-3045.
[27] J. Wood, L.F. Gladden, F.J. Keil, Modelling diffusion and reaction accompanied by capillary condensation using three-dimensional pore networks. Part 2. Dusty gas model and general reaction kinetics, Chem. Engineer. Sci. 57 (2002) 3047-3059.
[28] D.A.L. Holtham, G.P. Matthews, D.S. Scholefield, Measurement and simulation of void structure and hydraulic changes caused by root-induced soil structuring under white clover compared to ryegrass, Geoderma 142 (2007) 142-151.
[29] A. Gomez-Carracedo, R. Martinez-Pacheco, A. Concheiro, J.L. Gomez-Amoza, Modelling of porosity and waterfronts in cellulosic pellets for understanding drug release behavior, Int. J. Pharm. 388 (2010) 101-106.
[30] G. Mabilleau, M.F. Baslé, D. Chappard, Evaluation of surface roughness of hydrogels by fractal texture analysis during swelling, Langmuir 22 (2006) 4843-4845.
[31] D. Chappard, I. Degasne, G. Huré, E. Legrand, M. Audran, M.F. Baslé, Image analysis measurements of roughness by texture and fractal analysis correlate with contact profilometry, Biomaterials 24 (2003) 1399-1407.
[32] C. Ridgway, P. Gane, A. Abd, A. Czachor, Water absorption into construction materials: comparison of neutron radiography data with network absorption models, Transport Porous Med. 63 (2006) 503-525.
[33] A. Johnson, I.M. Roy, G.P. Matthews, D. Patel, An improved simulation of void structure, water retention and hydraulic conductivity in soil with the Pore-Cor three-dimensional network, Eur. J. Soil Sci. 54 (2003) 477-490.
[34] D.M.W. Peat, G.P. Matthews, P.J. Worsfold, S.C. Jarvis, Simulation of water retention and hydraulic conductivity in soil using a three-dimensional network, Eur. J. Soil Sci. 51 (2000) 65-79.
[35] R.K. Ahuja, M. Kodialam, A.K. Mishra, J.B. Orlin, Computational investigations of maximum flow algorithms, Eur. J. Oper. Res. 97 (1997) 509-542.
[36] S. Sudsakorn, L. Kaplan, D.A. Williams, Simultaneous determination of triamcinolone acetonide and oxymetazoline hydrochloride in nasal spray formulations by HPLC, J. Pharm. Biomed. Anal. 40 (2006) 1273-1280.

[37] G.V. Gupchup, J.L. Zatz, Structural characteristics and permeability properties of the human nail: A review, J. Cosmet. Sci. 50 (1999) 363-385.
[38] J.L. Pérez Bernal, M.A. Bello, Fractal geometry and mercury porosimetry: Comparison and application of proposed models on building stones, App. Surf. Sci. 185 (2001) 99-107.
[39] S. Wessel, M. Gniadecka, G.B.E. Jemec, H.C. Wulf, Hydration of human nails investigated by NIR-FT-Raman spectroscopy, BBA - Protein Struct. M. 1433 (1999) 210-216.
[40] M. Gniadecka, O.F. Nielsen, D.H. Christensen, H.C. Wulf, Structure of water, proteins, and lipids in intact human skin, hair, and nail, J. Invest. Dermatol. 110 (1998) 393-398.
[41] R.H. Khengar, S.A. Jones, R.B. Turner, B. Forbes, M.B. Brown, Nail swelling as a pre-formulation screen for the selection and optimisation of ungual penetration enhancers, Pharm. Res. 24 (2007) 2207-2212.
[42] Matthews G.P.; Moss, A.K. ; Spearing M.C. and Voland, F. Network calculation of mercury intrusion and absolute permeability in sandstone and other porous media. Powder Techmology 76 (1993) 95-107.
[43] J. Schoelkopf, P.A.C. Gane, C.J. Ridgway, A comparison of the various liquid interaction radii derived from experiment and network modelling of porous pigmented structures, Colloid Surface Physicochem. Eng. Aspect, 251 (2004) 149-159.